Communication

Linker Engineering toward Full-Color Emission of UiO-68 Type Metal−Organic Frameworks

Shenjie Wu, Daming Ren, Kang Zhou, Hai-Lun Xia, Xiao-Yuan Liu,* Xiaotai Wang, and Jing Li*

Read Online

ACCESS | ▮▮ Metrics & More | 📰 Article Recommendations | ⓢⓘ Supporting Information

ABSTRACT: Luminescent metal−organic frameworks (LMOFs) demonstrate strong potential for a broad range of applications due to their tunable compositions and structures. However, the methodical control of the LMOF emission properties remains a great challenge. Herein, we show that linker engineering is a powerful method for systematically tuning the emission behavior of UiO-68 type metal−organic frameworks (MOFs) to achieve full-color emission, using 2,1,3-benzothiadiazole and its derivative-based dicarboxylic acids as luminescent linkers. To address the fluorescence self-quenching issue caused by densely packed linkers in some of the resultant UiO-68 type MOF structures, we apply a mixed-linker strategy by introducing nonfluorescent linkers to diminish the self-quenching effect. Steady-state and time-resolved photoluminescence (PL) experiments reveal that aggregation-caused quenching can indeed be effectively reduced as a result of decreasing the concentration of emissive linkers, thereby leading to significantly enhanced quantum yield and increased lifetime.

Organic-linker-based luminescent metal−organic frameworks (LMOFs)[1] have been extensively studied for possible applications in sensing,[2] bioimaging,[3] and solid-state lighting.[4] However, two major challenges remain in developing such LMOFs: (i) how to develop a facile and universal approach to systematically tune the emission behavior of the resulting MOFs and (ii) how to effectively reduce aggregation-caused self-quenching in densely packed and rigid MOF structures.[4c,5] Linker engineering is a powerful strategy to confer specific properties or new functions on targeted MOFs,[6] which has been employed to improve MOF performance in catalysis,[7] biomedicine,[8] and other areas.[6a,9] However, no work has been reported on the use of this strategy to systematically study the relationship between the linker structure and the emission behavior in organic-linker-based LMOFs or to achieve full-color emission in these LMOFs. The starting point is to identify and use suitable organic compounds as a model to study the structure−emission relationships in the resulting LMOFs, which can provide valuable insights for the further development of LMOFs with tunable emission properties.

The bicyclic compound 2,1,3-benzothiadiazole and its analogues are a class of easily modifiable molecules.[10] As depicted in Scheme 1, their emission properties can be tuned via three functional sites to achieve full-color emission. On the other hand, UiO-68 is one of the most extensively studied MOFs, constructed by [1,1′:4′,1-terphenyl]-4,4″-dicarboxylic acid (TPDC) and Zr$_6$ clusters. Although some efforts have been made to prepare UiO-68 type LMOFs with functionalized TPDC for sensing,[2d,11] the tunability is very limited. Inspired by the tunable emission behavior of 2,1,3-benzothiadiazole and its analogues, we envision that replacing the center benzene ring of TPDC by 2,1,3-benzothiadiazole or its analogues (Scheme 1) not only will retain the topology of prepared MOFs but, more importantly, will also introduce

Scheme 1. Schematic Diagram Illustrating Linker Engineering Using 2,1,3-Benzothiadiazole (X = S) (Left) as a Core to Design Dicarboxylic Acid Based Organic Linkers (Right)
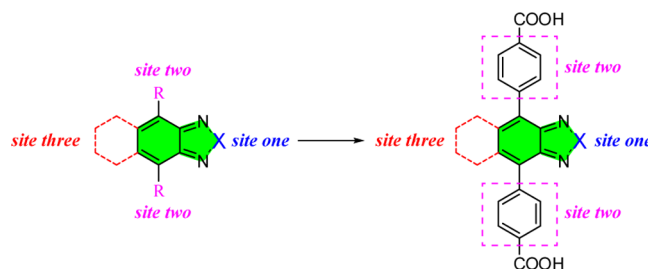

three functional sites, allowing a systematic and broad tunability of the emission properties of the resulting UiO-68 type MOFs. Such an approach may also be applied as a promising platform for constructing other LMOFs.

These ideas led us to design and synthesize six 2,1,3-benzothiadiazole-based linkers according to the aforementioned three modification sites by facile procedures under mild conditions, whose structures are shown in Figure 1a. These are 4,4′-(2H-benzo[d][1,2,3]triazole-4,7-diyl)bis(3-methoxybenzoic acid) (BAMB), 4,4′-(5,6-dimethylbenzo[c][1,2,5]-thiadiazole-4,7-diyl)dibenzoic acid (MBTB), 4,4′-(benzo[c]-[1,2,5]thiadiazole-4,7-diyl)bis(3-methoxybenzoic acid) (BTMB),[12] 4,4′-(benzo[c][1,2,5]selenadiazole-4,7-diyl)bis(3-
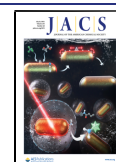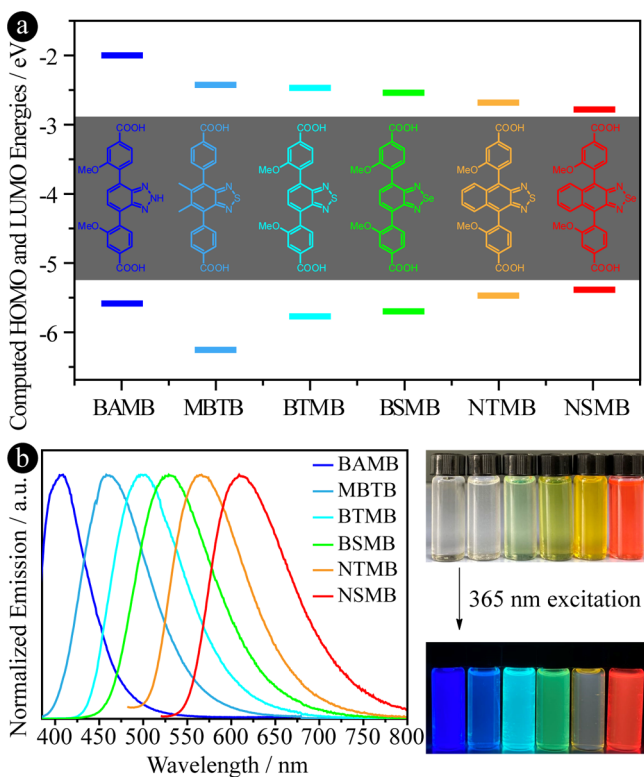
Figure 1. (a) Molecular structures and calculated HOMO−LUMO energy levels and (b) normalized fluorescence spectra and photographs of the samples in DMF under daylight and 365 nm excitation of BAMB, MBTB, BTMB, BSMB, NTMB, and NSMB.

methoxybenzoic acid) (BSMB), 4,4′-(naphtho[2,3-c][1,2,5]-thiadiazole-4,9-diyl)bis(3-methoxybenzoic acid) (NTMB), and 4,4′-(naphtho[2,3-c][1,2,5]selenadiazole-4,9-diyl) bis(3-methoxybenzoic acid) (NSMB). The molecular orbitals of these linkers were calculated using density functional theory (DFT). As depicted in Figure 1a, the lowest unoccupied molecular orbital (LUMO) energies gradually decrease along with increased highest occupied molecular orbital (HOMO) energies from BAMB to NSMB except for MBTB. As a result, the HOMO−LUMO energy gap is significantly decreased, which shows the enabling power of the three-site-based linker engineering to tune the electronic structures of the designed molecules.

To further prove our hypothesis, the steady-state emission and UV−vis absorption spectra of these organic linkers in N,N-dimethylformamide (DMF) solution were measured and are shown in Figure 1b and Figure S1. As expected, the emission energy varies from blue (BAMB) to red (NSMB), covering the full visible-light range, which is consistent with their UV−vis absorption spectra. The maximum emission peaks appear at 408, 460, 500, 530, 566, and 610 nm for BAMB, MBTB, BTMB, BSMB, NTMB, and NSMB, respectively. The corresponding colors under daylight and 365 nm excitation are also shown in Figure 1b. A closer look at the molecular structures reveals an interesting structure−emission correlation. (i) When the NH group on BAMB was replaced by S to form BTMB, a 92 nm bathochromic shift was observed. (ii) When two methyl groups were added to BTMB but two methoxy groups were removed, a 40 nm hypochromic shift was measured for MBTB. (iii) The single-atom substitution from S to Se resulted in a 30 nm red shift from BTMB to BSMB and a

44 nm red shift from NTMB to NSMB. In addition, (iv) extended conjugation also offers significant red shifts of 66 and 80 nm from BTMB to NTMB and from BSMB to NSMB, respectively. These results demonstrate that the three-site-based linker engineering indeed is a powerful strategy to systematically tune the emission properties of 2,1,3-benzothiadiazole-related dicarboxylic acids, which may be applied to other types of organic linkers to achieve a desirable emission color.

Single crystals of six UiO-68 type MOFs based on these organic linkers (Ls) were obtained by analogy to literature procedures.[11b] A typical synthesis of UiO-68-BTMB is schematically shown in Figure 2a: a 5 mL vial containing 3
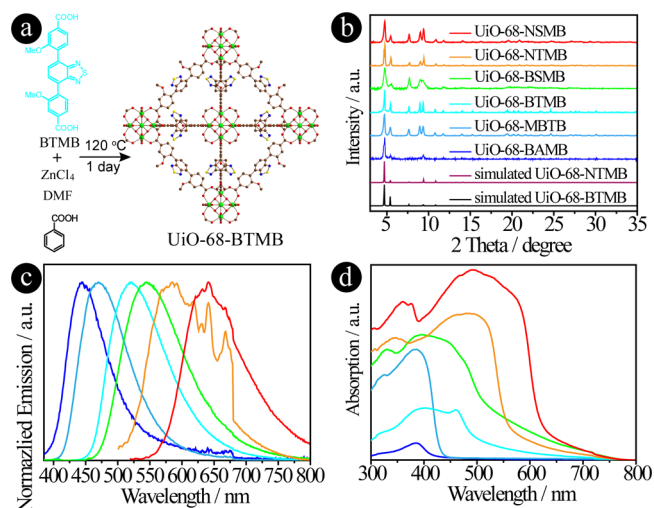

Figure 2. (a) Synthesis scheme for UiO-68 type MOFs using BTMB as the organic linker. (b) PXRD patterns, (c) normalized solid-state emission spectra, and (d) UV−vis absorption spectra of UiO-68-BAMB, UiO-68-MBTB, UiO-68-BTMB, UiO-68-BSMB, UiO-68-NTMB, and UiO-68-NSMB.

mL of DMF, ZrCl$_4$ (11.2 mg, 0.048 mmol), BTMB (30.5 mg, 0.070 mmol), and benzoic acid (222.6 mg, 1.82 mmol) was placed in a preheated oven at 120 °C for 24 h. Depending on the properties of the organic linkers, colorless (UiO-68-BAMB), colorless (UiO-68-MBTB), light yellow (UiO-68-BTMB), yellow (UiO-68-BSMB), orange (UiO-68-NTMB), and dark red (UiO-68-NSMB) octagonal-shaped single crystals were obtained (Figure S2). The powder X-ray diffraction (PXRD) patterns of the UiO-68-L samples match well with those of the simulated UiO-68-BTMB and UiO-68-NTMB (Figure 2b), indicating that the six linkers with various degrees of modifications (including large molecular structures such as NTMB and NSMB) give rise to the same isoreticular series with the same topology as for UiO-68.

UiO-68-BAMB, UiO-68-MBTB, UiO-68-BTMB, and UiO-68-BSMB give emissions at different colors with their peak maxima at 445 nm (deep blue), 470 nm (light blue), 520 nm (cyan), and 545 nm (light green), respectively (Figure 2c). The corresponding solid-state photoluminescence quantum yields (PLQYs) are 5.80%, 14.6%, 36.0%, and 2.80%, respectively, which are much higher than those of the corresponding linkers (0.60%, 5.50%, 1.50%, and 0.30%). The enhanced PLQYs can be attributed to the fact that the immobilization and separation of the linkers into MOF backbone effectively prevents them from aggregation, thus

greatly suppressing aggregation-caused quenching (ACQ) effects.[13] However, UiO-68-NTMB and UiO-68-NSMB give much weaker emission with very low PLQYs of 0.30% and 0.70%, respectively, comparable to those of their corresponding linkers (0.40% and 0.10%). The very low PLQYs of the two linkers and the associated MOFs are due to the close linker–linker distances and relatively strong π–π stacking interactions, which lead to a substantial ACQ effect, in contrast with the other four smaller linkers and their MOFs.[13] The UV–vis spectra of the six MOFs are generally consistent with their HOMO–LUMO gaps and emission energies (Figure 2d). DFT calculations on the fragments of UiO-68-NTMB and UiO-68-BTMB show that no significant changes are observed in the HOMO and LUMO orbitals in comparison with those of the corresponding linkers,[14] suggesting that the emission is linker-based (Figures S3 and S4).

To verify our speculation about the ACQ effect in UiO-68-NTMB and UiO-68-NSMB and to improve the quantum efficiency, a mixed-linker strategy was employed, where a nonemissive linker, 2′,5′-dimethyl-[1,1′:4′,1″-terphenyl]-4,4″-dicarboxylic acid (dTPDC), was used along with the emissive NTMB and NSMB to increase the distances between the emissive linkers.[5,10d,15] For dTPDC, its HOMO (LUMO) is much lower (higher) than those of the six emissive linkers; therefore, no charge/energy transfer will occur between dTPDC and the emissive linkers (Figure S5). Mixed-linker MOFs were thus prepared using the same method as for pure linker MOFs (Table S1), where the ratio of L and dTPDC varies from 1:1 to 1:2, 1:5, and 1:10. As depicted in Figure 3a, the PXRD patterns of all UiO-68-NTMB/dTPDC samples are nearly identical with that of the simulated UiO-68, indicative of the retention of the pristine structure even after mixing with increased concentrations of dTPDC. The solid-state emission spectra of four UiO-68-NTMB/dTPDC samples show slightly hypsochromic shifts with an increased concentration of dTPDC (Figure 3b), which might be attributed to the decreased concentration of lower-energy trap states.[4c,5] The increased concentration of dTPDC had a significant effect on the UV–vis absorption spectra of UiO-68-NTMB/dTPDC, in which the spectra exhibit a gradual blue shift with decreased intensity (Figure S6). This result could be ascribed to the fact that UiO-68-dTPDC has a weak and narrow absorption band in the visible-light range in comparison with UiO-68-NTMB (Figure S7). Transient fluorescence decay profiles of UiO-68-NTMB/dTPDC samples are presented in Figure 3c. It is very difficult to record the decay traces for pure UiO-68-NTMB and the sample with a 1:1 ratio of NTMB and dTPDC due to their extremely low PL intensity. However, with a decreased concentration of NTMB from 1:2 to 1:10, the lifetime is significantly increased from 6.90 to 16.0 ns, indicating that increasing the concentration of dTPDC has a remarkable effect on the excited-state properties of NTMB. The PLQY shows a significant improvement from 0.30% to 0.70%, 1.70%, 11.4%, and 18.8% with the decrease in the molar ratio for NTMB:dTPDC from 1:0 to 1:10, giving a 62.6 times enhancement. The remarkable suppression of ACQ by the mixed-linker strategy could be clearly observed by the naked eye as a result of the significantly enhanced emission of UiO-68-NTMB/dTPDC under 365 nm excitation (Figure 3d). It is apparent that the total nonradiative decay rates of UiO-68-NTMB/dTPDC gradually decreased with increased concentraion of dTPDC, which demonstrates that the nonradiative decay channels caused by aggregation can be effectively
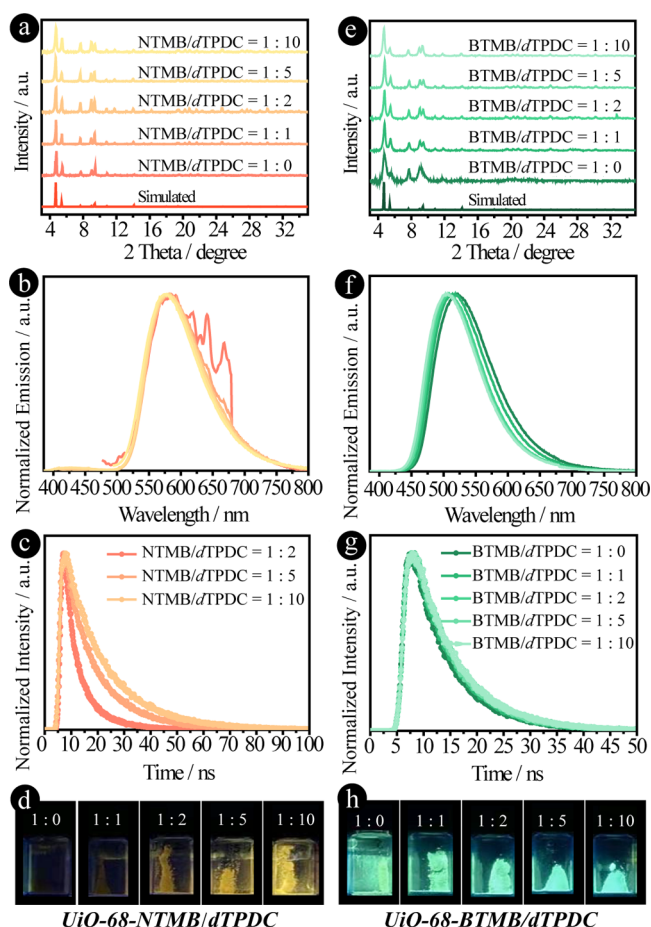

Figure 3. (a, e) PXRD patterns, (b, f) normalized solid-state emission spectra, (c, g) transient fluorescence decay profiles, and (d, h) photographs under 365 nm excitation of mixed-linkers UiO-68-NTMB/dTPDC and UiO-68-BTMB/dTPDC with different concentrations of dTPDC.

reduced via combining the nonemissive dTPDC into the crystal structures (Table S2). Similar photophysical properties were observed for UiO-68-NSMB/dTPDC, as NSMB has nearly the same molecular size as NTMB (Figure S8), where the enhancement of PLQY is 21.0 times.

To confirm that the photoluminescence self-quenching occurring in UiO-68-NTMB and UiO-68-NSMB was indeed related to the molecular size, we also synthesized the mixed-linker UiO-68-BTMB/dTPDC with various concentrations of dTPDC. All of the synthesized UiO-68-BTMB/dTPDC exhibit almost identical PXRD patterns with that of simulated UiO-68 (Figure 3e). Although the PL and UV–vis absorption spectra show similar changes with UiO-68-NTMB/dTPDC (Figure 3f and Figure S6), a slight change was measured for the transient fluorescence decay profiles, which demonstrates that the introduction of dTPDC has a limited effect on the excited state of UiO-68-BTMB/dTPDC (Figure 3g). The PLQYs of UiO-68-BTMB/dTPDC only change 1.56 times from 36.0% to 40.4%, 44.3%, 56.2%, and 47.8% with the variation of the molar ratio for BTMB:dTPDC from 1:0 to 1:10, which is very difficult to distinguish by the naked eye (Figure 3h). In addition, no significant changes were observed for the temperature-dependent emission and transient fluorescence decay profiles of UiO-68-BTMB/dTPDC from 293 to 77 K (Figure S9), indicating that the temperature effect on the

photochemistry of UiO-68-BTMB/dTPDC is very limited. Similar photophysical phenomena were observed for UiO-68-MBTB/dTPDC and UiO-68-BSMB/dTPDC with 1.67 and 3.10 times PLQY enhancement due to their similar molecular structures (Figures S10 and S11). The real ratios for BTMB and dTPDC in the mixed-linker UiO-68-BTMB/dTPDC samples were quantified by ^{1}H NMR on digested MOF samples (Figures S12−S16), which are very close to the ratios used in the actual synthesis.

The clear dependence of enhanced PLQYs and excited-state lifetimes on different dTPDC concentrations in UiO-68-NTMB/dTPDC and UiO-68-BTMB/dTPDC confirmed the presence of PL self-quenching of NTMB and BTMB in both MOF matrices. Partially replacing the emissive linkers by dTPDC effectively increases the NTMB−NTMB or BTMB−BTMB distances in UiO-68-NTMB/dTPDC and UiO-68-BTMB/dTPDC, thus reducing $\pi-\pi$ stacking interactions and, consequently, the ACQ effect.[13] In addition, an amplified self-quenching affect was observed in solid-state NTMB, NSMB, UiO-68-NTMB, and UiO-68-NSMB due to their larger molecular sizes in comparison to the other four linkers. Since the mixed-linker strategy directly affects the distance between the two emissive centers to tune the aggregation, the self-quenching mechanism in these compounds can be ascribed to ACQ. This can be further confirmed by analyzing the crystal structures of UiO-68-BTMB and UiO-68-NTMB (Figure 4
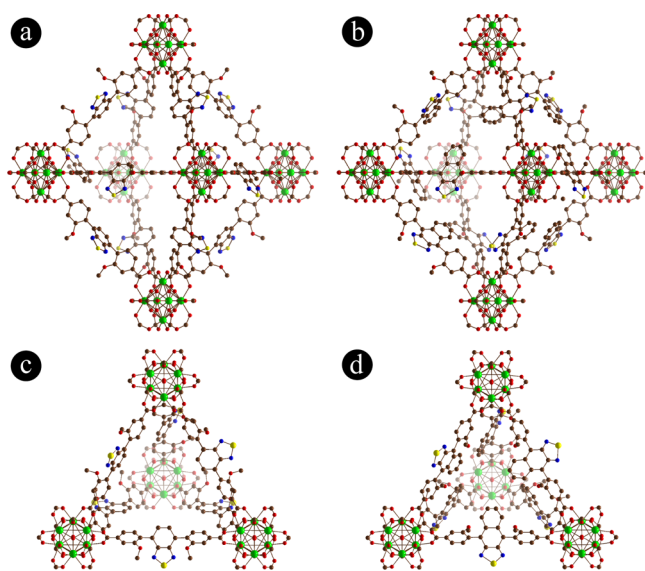

Figure 4. Single-crystal structures of UiO-68-BTMB (a, b) and UiO-68-NTMB (c, d) with octahedral (a, c) and tetrahedral (b, d) cavities.

and Table S3 and S4). For UiO-68 type MOFs, linkers are incorporated into large octahedral cavities and small tetrahedral cavities. On the basis of the reported data, the average distance between skeletons of the two linkers in octahedral and tetrahedral cavities are approximately 1.2−1.7 and 1.2−2.4 nm, respectively, while efficient energy transfer occurs when the distance is less than 1.7 nm and the emission from the donor can be significantly quenched.[10d] After another benzene ring is added to BTMB to form NTMB, the distance between two NTMBs in the rigid UiO-68 matrix will be further decreased and the two kinds of cavities become more crowded. As a result, a remarkable self-quenching occurs. After NTMB is replaced with increased concentrations of nonfluorescent

dTPDC, the distance between the two NTMBs will gradually increase and the ACQ will be suppressed, giving rise to an enhanced quantum yield.

In conclusion, linker engineering has been used to synthesize a series of 2,1,3-benzothiadiazole and its derivative-based dicarboxylic acid linkers, which can be employed to form a series of UiO-68 type MOFs with systematically tunable fluorescence covering the full color spectrum. In addition, applying the mixed-linker strategy allows us to make use of nonfluorescent linkers to significantly reduce the aggregation-caused quenching in densely packed MOFs matrices, thus greatly enhancing the emission efficiency. This approach is highly general and can be easily extended to other linker systems to facilitate the development of well-functionalized LMOFs.

■ ASSOCIATED CONTENT

Ⓢ Supporting Information

The Supporting Information is available free of charge at https://pubs.acs.org/doi/10.1021/jacs.1c04810.

> Materials, organic linker and MOF synthesis, ^{1}H NMR spectra, photoluminescent and UV−vis absorption spectra, PXRD, and other additional information (PDF)

Accession Codes

CCDC 2082073−2082074 contain the supplementary crystallographic data for this paper. These data can be obtained free of charge via www.ccdc.cam.ac.uk/data_request/cif, or by emailing data_request@ccdc.cam.ac.uk, or by contacting The Cambridge Crystallographic Data Centre, 12 Union Road, Cambridge CB2 1EZ, UK; fax: +44 1223 336033.

■ AUTHOR INFORMATION

Corresponding Authors

Xiao-Yuan Liu − *Hoffmann Institute of Advanced Materials, Shenzhen Polytechnic, Shenzhen 518055, People's Republic of China;* ⓞ orcid.org/0000-0003-2400-8085; Email: liuxiaoyuan1989@szpt.edu.cn

Jing Li − *Department of Chemistry and Chemical Biology, Rutgers University, Piscataway, New Jersey 08854, United States; Hoffmann Institute of Advanced Materials, Shenzhen Polytechnic, Shenzhen 518055, People's Republic of China;* ⓞ orcid.org/0000-0001-7792-4322; Email: jingli@rutgers.edu

Authors

Shenjie Wu − *Hoffmann Institute of Advanced Materials, Shenzhen Polytechnic, Shenzhen 518055, People's Republic of China*

Daming Ren − *Hoffmann Institute of Advanced Materials, Shenzhen Polytechnic, Shenzhen 518055, People's Republic of China*

Kang Zhou − *Hoffmann Institute of Advanced Materials, Shenzhen Polytechnic, Shenzhen 518055, People's Republic of China*

Hai-Lun Xia − *Hoffmann Institute of Advanced Materials, Shenzhen Polytechnic, Shenzhen 518055, People's Republic of China*

Xiaotai Wang − *Hoffmann Institute of Advanced Materials, Shenzhen Polytechnic, Shenzhen 518055, People's Republic of China; Department of Chemistry, University of Colorado*

Denver, Denver, Colorado 80217-3364, United States;
  orcid.org/0000-0003-3310-3308

REFERENCES

(1) (a) Allendorf, M. D.; Bauer, C. A.; Bhakta, R. K.; Houk, R. J. Luminescent metal-organic frameworks. *Chem. Soc. Rev.* **2009**, *38* (5), 1330. (b) Cui, Y.; Yue, Y.; Qian, G.; Chen, B. Luminescent Functional Metal−Organic Frameworks. *Chem. Rev.* **2012**, *112* (2), 1126. (c) Liu, X.-Y.; Lustig, W. P.; Li, J. Functionalizing Luminescent Metal−Organic Frameworks for Enhanced Photoluminescence. *ACS Energy Lett.* **2020**, *5* (8), 2671. (d) Martin, C. R.; Kittikhunnatham, P.; Leith, G. A.; Berseneva, A. A.; Park, K. C.; Greytak, A. B.; Shustova, N. B. Let the light be a guide: Chromophore communication in metal-organic frameworks. *Nano Res.* **2021**, *14* (2), 338.

(2) (a) Lustig, W. P.; Mukherjee, S.; Rudd, N. D.; Desai, A. V.; Li, J.; Ghosh, S. K. Metal-organic frameworks: functional luminescent and photonic materials for sensing applications. *Chem. Soc. Rev.* **2017**, *46* (11), 3242. (b) Lan, A.; Li, K.; Wu, H.; Olson, D. H.; Emge, T. J.; Ki, W.; Hong, M.; Li, J. A Luminescent Microporous Metal−Organic Framework for the Fast and Reversible Detection of High Explosives. *Angew. Chem., Int. Ed.* **2009**, *48* (13), 2334. (c) Hu, Z.; Lustig, W. P.; Zhang, J.; Zheng, C.; Wang, H.; Teat, S. J.; Gong, Q.; Rudd, N. D.; Li, J. Effective Detection of Mycotoxins by a Highly Luminescent Metal-Organic Framework. *J. Am. Chem. Soc.* **2015**, *137* (51), 16209. (d) Mallick, A.; El-Zohry, A. M.; Shekhah, O.; Yin, J.; Jia, J.; Aggarwal, H.; Emwas, A. H.; Mohammed, O. F.; Eddaoudi, M. Unprecedented Ultralow Detection Limit of Amines using a Thiadiazole-Functionalized Zr(IV)-Based Metal-Organic Framework. *J. Am. Chem. Soc.* **2019**, *141* (18), 7245. (e) Hu, Z.; Deibert, B. J.; Li, J. Luminescent metal-organic frameworks for chemical sensing and explosive detection. *Chem. Soc. Rev.* **2014**, *43* (16), 5815. (f) Zhao, Y.; Zeng, H.; Zhu, X.-W.; Lu, W.; Li, D. Metal−organic frameworks as photoluminescent biosensing platforms: mechanisms and applications. *Chem. Soc. Rev.* **2021**, *50*, 4484.

(3) (a) Park, J.; Jiang, Q.; Feng, D.; Mao, L.; Zhou, H. C. Size-Controlled Synthesis of Porphyrinic Metal-Organic Framework and Functionalization for Targeted Photodynamic Therapy. *J. Am. Chem. Soc.* **2016**, *138* (10), 3518. (b) Park, J.; Xu, M.; Li, F.; Zhou, H. C. 3D Long-Range Triplet Migration in a Water-Stable Metal-Organic Framework for Upconversion-Based Ultralow-Power in Vivo Imaging. *J. Am. Chem. Soc.* **2018**, *140* (16), 5493.

(4) (a) Gong, Q.; Hu, Z.; Deibert, B. J.; Emge, T. J.; Teat, S. J.; Banerjee, D.; Mussman, B.; Rudd, N. D.; Li, J. Solution Processable MOF Yellow Phosphor with Exceptionally High Quantum Efficiency. *J. Am. Chem. Soc.* **2014**, *136* (48), 16724. (b) Cornelio, J.; Zhou, T.-Y.; Alkaş, A.; Telfer, S. G. Systematic Tuning of the Luminescence Output of Multicomponent Metal−Organic Frameworks. *J. Am. Chem. Soc.* **2018**, *140* (45), 15470. (c) Newsome, W. J.; Ayad, S.; Cordova, J.; Reinheimer, E. W.; Campiglia, A. D.; Harper, J. K.; Hanson, K.; Uribe-Romo, F. J. Solid State Multicolor Emission in Substitutional Solid Solutions of Metal−Organic Frameworks. *J. Am. Chem. Soc.* **2019**, *141*, 11298. (d) Lustig, W. P.; Shen, Z.; Teat, S. J.; Javed, N.; Velasco, E.; O'Carroll, D. M.; Li, J. Rational design of a high-efficiency, multivariate metal−organic framework phosphor for

white LED bulbs. *Chem. Sci.* **2020**, *11* (7), 1814. (e) Lustig, W. P.; Li, J. Luminescent metal−organic frameworks and coordination polymers as alternative phosphors for energy efficient lighting devices. *Coord. Chem. Rev.* **2018**, *373*, 116.

(5) Chakraborty, A.; Ilic, S.; Cai, M.; Gibbons, B. J.; Yang, X.; Slamowitz, C. C.; Morris, A. J. Role of Spin−Orbit Coupling in Long Range Energy Transfer in Metal−Organic Frameworks. *J. Am. Chem. Soc.* **2020**, *142* (48), 20434.

(6) (a) Deng, H.; Doonan, C. J.; Furukawa, H.; Ferreira, R. B.; Towne, J.; Knobler, C. B.; Wang, B.; Yaghi, O. M. Multiple functional groups of varying ratios in metal-organic frameworks. *Science* **2010**, *327* (5967), 846. (b) Deng, H.; Grunder, S.; Cordova, K. E.; Valente, C.; Furukawa, H.; Hmadeh, M.; Gandara, F.; Whalley, A. C.; Liu, Z.; Asahina, S.; Kazumori, H.; O'Keeffe, M.; Terasaki, O.; Stoddart, J. F.; Yaghi, O. M. Large-pore apertures in a series of metal-organic frameworks. *Science* **2012**, *336* (6084), 1018.

(7) (a) Chen, D.; Yang, W.; Jiao, L.; Li, L.; Yu, S.-H.; Jiang, H.-L. Boosting Catalysis of Pd Nanoparticles in MOFs by Pore Wall Engineering: The Roles of Electron Transfer and Adsorption Energy. *Adv. Mater.* **2020**, *32* (30), 2000041. (b) Lionet, Z.; Kim, T.-H.; Horiuchi, Y.; Lee, S. W.; Matsuoka, M. Linker Engineering of Iron-Based MOFs for Efficient Visible-Light-Driven Water Oxidation Reaction. *J. Phys. Chem. C* **2019**, *123* (45), 27501.

(8) Wu, J.; Yu, Y.; Cheng, Y.; Cheng, C.; Zhang, Y.; Jiang, B.; Zhao, X.; Miao, L.; Wei, H. Ligand-Dependent Activity Engineering of Glutathione Peroxidase-Mimicking MIL-47(V) Metal−Organic Framework Nanozyme for Therapy. *Angew. Chem., Int. Ed.* **2021**, *60* (3), 1227.

(9) (a) Hendon, C. H.; Tiana, D.; Fontecave, M.; Sanchez, C.; D'arras, L.; Sassoye, C.; Rozes, L.; Mellot-Draznieks, C.; Walsh, A. Engineering the Optical Response of the Titanium-MIL-125 Metal−Organic Framework through Ligand Functionalization. *J. Am. Chem. Soc.* **2013**, *135* (30), 10942. (b) Liu, L.; Yao, Z.; Ye, Y.; Yang, Y.; Lin, Q.; Zhang, Z.; O'Keeffe, M.; Xiang, S. Integrating the Pillared-Layer Strategy and Pore-Space Partition Method to Construct Multi-component MOFs for C2H2/CO2 Separation. *J. Am. Chem. Soc.* **2020**, *142* (20), 9258.

(10) (a) Neto, B. A. D.; Lapis, A. A. M.; da Silva Júnior, E. N.; Dupont, J. 2,1,3-Benzothiadiazole and Derivatives: Synthesis, Properties, Reactions, and Applications in Light Technology of Small Molecules. *Eur. J. Org. Chem.* **2013**, *2013* (2), 228. (b) Chen, L.; Wang, L.; Jing, X.; Wang, F. Color tuning of Novel 2,1,3-Naphthothiadiazole and 2,1,3-Benzoselenadiazole based D-A-D′ Type dopants to realize highly efficient saturated red emission in non-polar solvents. *J. Mater. Chem.* **2011**, *21* (28), 10265. (c) Benson, S.; Fernandez, A.; Barth, N. D.; de Moliner, F.; Horrocks, M. H.; Herrington, C. S.; Abad, J. L.; Delgado, A.; Kelly, L.; Chang, Z.; Feng, Y.; Nishiura, M.; Hori, Y.; Kikuchi, K.; Vendrell, M. SCOTfluors: Small, Conjugatable, Orthogonal, and Tunable Fluorophores for In Vivo Imaging of Cell Metabolism. *Angew. Chem., Int. Ed.* **2019**, *58* (21), 6911. (d) Jia, J.; Gutiérrez-Arzaluz, L.; Shekhah, O.; Alsadun, N.; Czaban-Jóźwiak, J.; Zhou, S.; Bakr, O. M.; Mohammed, O. F.; Eddaoudi, M. Access to Highly Efficient Energy Transfer in Metal−Organic Frameworks via Mixed Linkers Approach. *J. Am. Chem. Soc.* **2020**, *142* (19), 8580.

(11) (a) Zhang, W.-Q.; Li, Q.-Y.; Cheng, J.-Y.; Cheng, K.; Yang, X.; Li, Y.; Zhao, X.; Wang, X.-J. Ratiometric Luminescent Detection of Organic Amines Due to the Induced Lactam−Lactim Tautomerization of Organic Linker in a Metal−Organic Framework. *ACS Appl. Mater. Interfaces* **2017**, *9* (37), 31352. (b) Gui, B.; Meng, X.; Chen, Y.; Tian, J.; Liu, G.; Shen, C.; Zeller, M.; Yuan, D.; Wang, C. Reversible Tuning Hydroquinone/Quinone Reaction in Metal−Organic Framework: Immobilized Molecular Switches in Solid State. *Chem. Mater.* **2015**, *27* (18), 6426. (c) Li, Y.-A.; Yang, S.; Li, Q.-Y.; Ma, J.-P.; Zhang, S.; Dong, Y.-B. UiO-68-ol NMOF-Based Fluorescent Sensor for Selective Detection of HClO and Its Application in Bioimaging. *Inorg. Chem.* **2017**, *56* (21), 13241. (d) Gui, B.; Meng, Y.; Xie, Y.; Tian, J.; Yu, G.; Zeng, W.; Zhang, G.; Gong, S.; Yang, C.; Zhang, D.; Wang, C. Tuning the Photoinduced Electron Transfer in a Zr-MOF:

Toward Solid-State Fluorescent Molecular Switch and Turn-On Sensor. *Adv. Mater.* **2018**, *30* (34), 1802329.

(12) Angioni, E.; Marshall, R. J.; Findlay, N. J.; Bruckbauer, J.; Breig, B.; Wallis, D. J.; Martin, R. W.; Forgan, R. S.; Skabara, P. J. Implementing fluorescent MOFs as down-converting layers in hybrid light-emitting diodes. *J. Mater. Chem. C* **2019**, *7* (8), 2394.

(13) (a) Förster, T.; Kasper, K. Ein Konzentrationsumschlag der Fluoreszenz. *Z. Phys. Chem. (Muenchen, Ger.)* **1954**, *1*, 275. (b) Briks, J. B. *Photophysics of Aromatic Molecules*; Wiley: London, 1970.

(14) (a) Wei, P.; Duan, L.; Zhang, D.; Qiao, J.; Wang, L.; Wang, R.; Dong, G.; Qiu, Y. A new type of light-emitting naphtho[2,3-c][1,2,5]thiadiazole derivatives: synthesis, photophysical characterization and transporting properties. *J. Mater. Chem.* **2008**, *18* (7), 806. (b) Angioni, E.; Chapran, M.; Ivaniuk, K.; Kostiv, N.; Cherpak, V.; Stakhira, P.; Lazauskas, A.; Tamulevičius, S.; Volyniuk, D.; Findlay, N. J.; Tuttle, T.; Grazulevicius, J. V.; Skabara, P. J. A single emitting layer white OLED based on exciplex interface emission. *J. Mater. Chem. C* **2016**, *4* (17), 3851.

(15) Newsome, W. J.; Chakraborty, A.; Ly, R. T.; Pour, G. S.; Fairchild, D. C.; Morris, A. J.; Uribe-Romo, F. J. J-dimer emission in interwoven metal−organic frameworks. *Chem. Sci.* **2020**, *11* (17), 4391.